ORIGINAL RESEARCH ARTICLE

MODIFICATION OF THERMAL HYDRAULIC TRANSIENT MODELS FOR THE MINIATURE NEUTRON SOURCE REACTOR

N. Abubakar[1, 2*], I. Garba[1], and M. T. Jimoh[1]

[1]Department of Mechanical Engineering, Bayero University, Kano, Nigeria
[2]Centre for Energy Research and Training, Ahmadu Bello University, Zaria, Nigeria)
*Corresponding author's email address: nabubakar@abu.edu.ng

ARTICLE INFORMATION	ABSTRACT

A modified Miniature Neutron Source Reactor (MNSR) model dealing with transient thermal hydraulic problem is presented. The model based on lumped parameter method is adopted in this work to numerically solve a system of coupled algebraic and differential equations governing heat transfer in MNSR, using MATLAB solver for variable order method in stiff differential equations and Differential-Algebraic equations, coupled with Maple soft. The simulated results obtained from the model were generally in agreement when compared with reactor operation data recorded from 0 to 270 minutes during experiments. Radiating energy of Fuel and clad and heat transferred at the gap or clearance were taken in to account. Fuel and clad temperatures as well as various temperatures at different sections of the reactor were predicted with the model, in addition to the effect of the installed chiller on the reactor coolant.

1.0 Introduction

Analysis of transient behaviour of research reactors is significantly relevant in the determination of the safety limits and margins imposed by fuel and clad melting temperatures as well as boiling temperature of the coolant (Anglart, 2011; Abubakar and Yahaya, 2012).

Miniature Neutron Source Reactor (MNSR) is a tank-in-pool reactor. The core of the reactor is immersed in the tank (reactor vessel) which is immersed in a large pool of water as shown schematically in Figure 1. It uses Uranium-Aluminum alloy as fuel with an in-core inventory of about 1kg of 90.2% enriched uranium, thick metallic beryllium surrounding the core as reflector and light water as coolant and moderator. MNSR has a nominal power of approximately 30 kW. The heat generated by the fuel is being removed by natural convection heat transfer process from the core to the pool. Under normal reactor operating conditions, it is expected that the rate of heat generation in the fuel will be the same as the rate of heat removal by the coolant.

The reactor small core is designed to be compact, safe, and to maintain a stable neutron flux for neutron activation analysis which is the principal utilization of the reactor. It is also used for production of short-lived radioisotopes and for education and training (Yongchun et al., 1992).

The previous simplified MNSR Thermal Hydraulics models described (Zhang, 1993; Albarhoum and Mohammed, 2009; Yamoah et al., 2011) did not include the fuel heat transfer process model from the fuel pellet to the clad involving expression for estimating the fuel temperature, but instead assumed an approximate value of 1°C difference between the fuel and clad temperatures and therefore neglect the difference and assume same temperature at any point and time for both fuel and clad. In addition, they did not account for the eventuality of existence of a very small non uniform space or gap between the fuel and clad (Quian, 1990). These models were over simplified as this study shows that the difference in temperature could not necessarily be as assumed previously.

Zang, 1993 model could not take into account the eventuality of cooling some parts of the tank vessel) or the pool of the reactor by cooling coil or chiller. Albarhum and Mohammed (2009), and Yamoah et al. (2011) models considered the effect of the cooling coil in the pool and the upper section of the reactor vessel, while all the previous models could not account for the gap resistance and fuel temperature estimation. It was assumed that at any power level attained during transients, the temperature at the fuel and cladding regions will be the same (Quian, 1990; Yamoah, et al., 2011) neglecting the thermal resistance expected between the pellet and the clad. Because the clad is a tube in which the fuel pellet is inserted, as a result there exist a small non-uniform gap which should be accounted for. Even though MNSR fuel rods are very small, it is true that that there exists a minute empty gap in the tube (Saha et al., 2013). With the conversion of MNSR fuel for HEU to LEU, the fuel-clad gap may be wider due inclusion of an inert gas in the gap to take care of the apparent expansion of LEU during operation; hence the need for this work to achieve sufficiently precise outputs.

The previous models were modified using the configuration of the Nigeria MNSR (NIRR-1) whose nominal power is 31 kW (Dim et al., 2012) and applies to structurally similar reactors, taking in to cognisance that some features in the structural design of the reactor and behavior of the power rise up time to its operational level may differ from one MNSR to another. The modification is also dependent on the reactor structure as such takes no account of reactivity insertions. Radiating energies from the fuel, gap and clad are also taken into account and calculated. This work specifically considers the gap clearance which exist between the fuel pellet to predict the true representation of the fuel and clad temperatures separately and this modifies the previous MNSR models that assumed and lumped the fuel and clad temperatures as approximately the same.

This paper modifies the previous MNSR thermal hydraulic models to provide a more accurate predictive tool which is necessary and important for obtaining information to ensure the safety of the reactor when making modifications (IAEA, 2001). MATLAB software was employed to model and simulate the MNSR natural convection coolant flow which depends on the coolant density difference due to temperature changes and pressure drop in the core which depends on the fuel elements grids in the core structure. Parameters studied are fuel and clad temperatures, coolant average temperatures at the core inlet, core outlet, core (bulk) and pool, and the coolant upward flow velocity in the reactor core. The model was validated by comparing with the experimental data and used to simulate and study other reactor parameters at nominal reactor power such as fuel temperature and effect of the cooling coil installed around the vessel in the reactor pool.
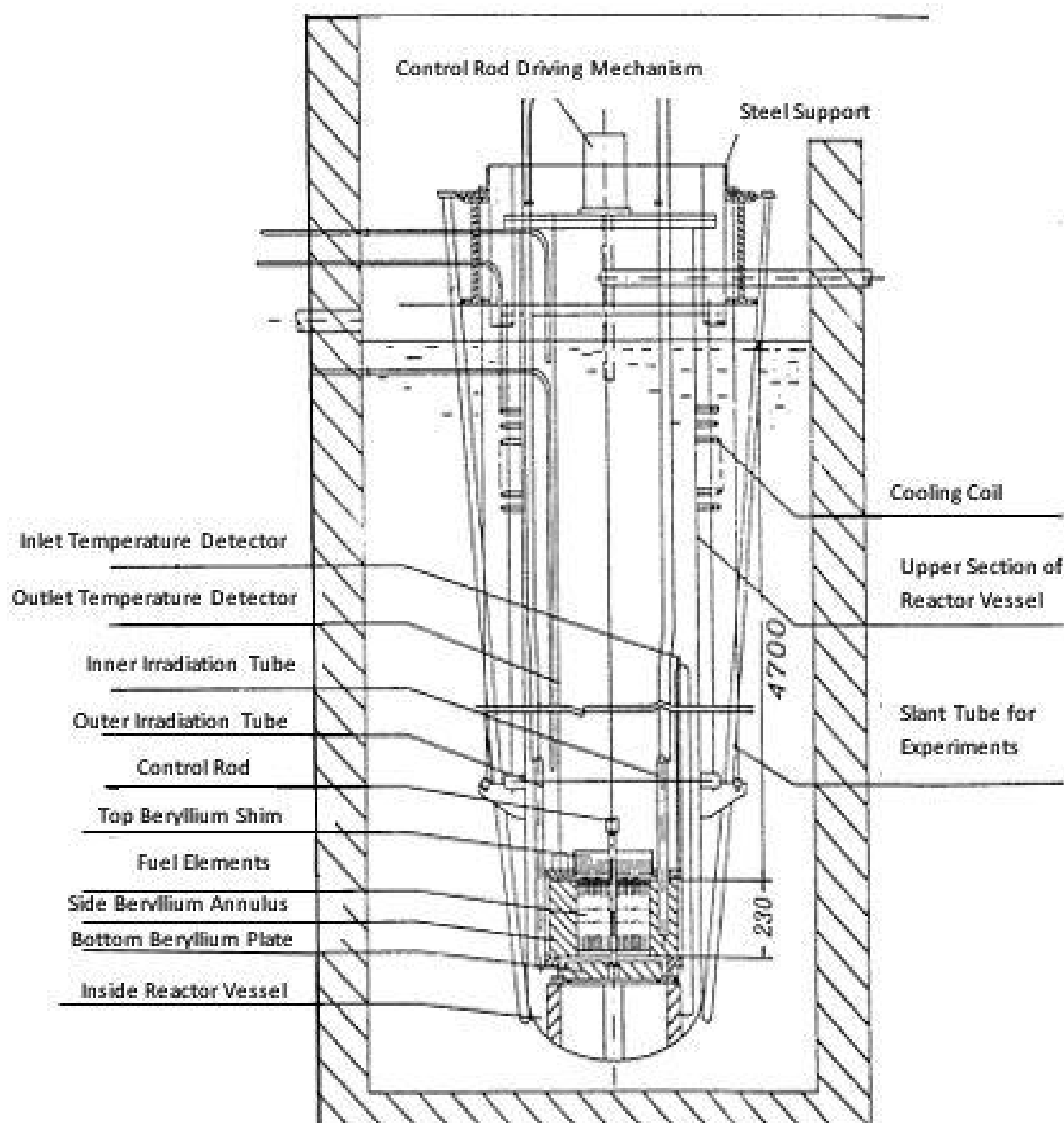
Figure 1: Vertical cross-section of MNSR assembly

2. Materials and Methods

To develop the generic MNSR thermal hydraulic model for the natural convection, the practical and theoretical data available including structural information were obtained. Some required data were generated through experiments using NIRR-1, and by estimations and assumptions. These data were used to develop the systems of mathematical expressions that form the model. The expressions were coupled together and solved numerically using MATLAB to simulate and validate the model behaviour. During the validation process, comparison of results was carried out between the simulated results and the data obtained through experiments.

2.1 Reactor core coolant flow pattern in MNSR

The flow pattern for the MNSR shown schematically in Figure 2 depicts the natural (circulation) convection of the coolant within the core area in the vessel. The process is established with the

generation of heat by fission occurring within the fuel elements in the core. The coolant moves up along the cladded walls of the fuel elements through the channels in the core and leaves it through the apertures surrounding the grids of the fuel elements to the outlet orifice, after which the coolant mixes with the water in the upper part of the vessel. Cold coolant from the bottom replaces the hot one leaving the core by siphoning effect causing the coolant in the down-comer (side of beryllium annulus) to move downwards at a maintained temperature and enters the reactor core at the inlet orifice (Wuqin, 1997).
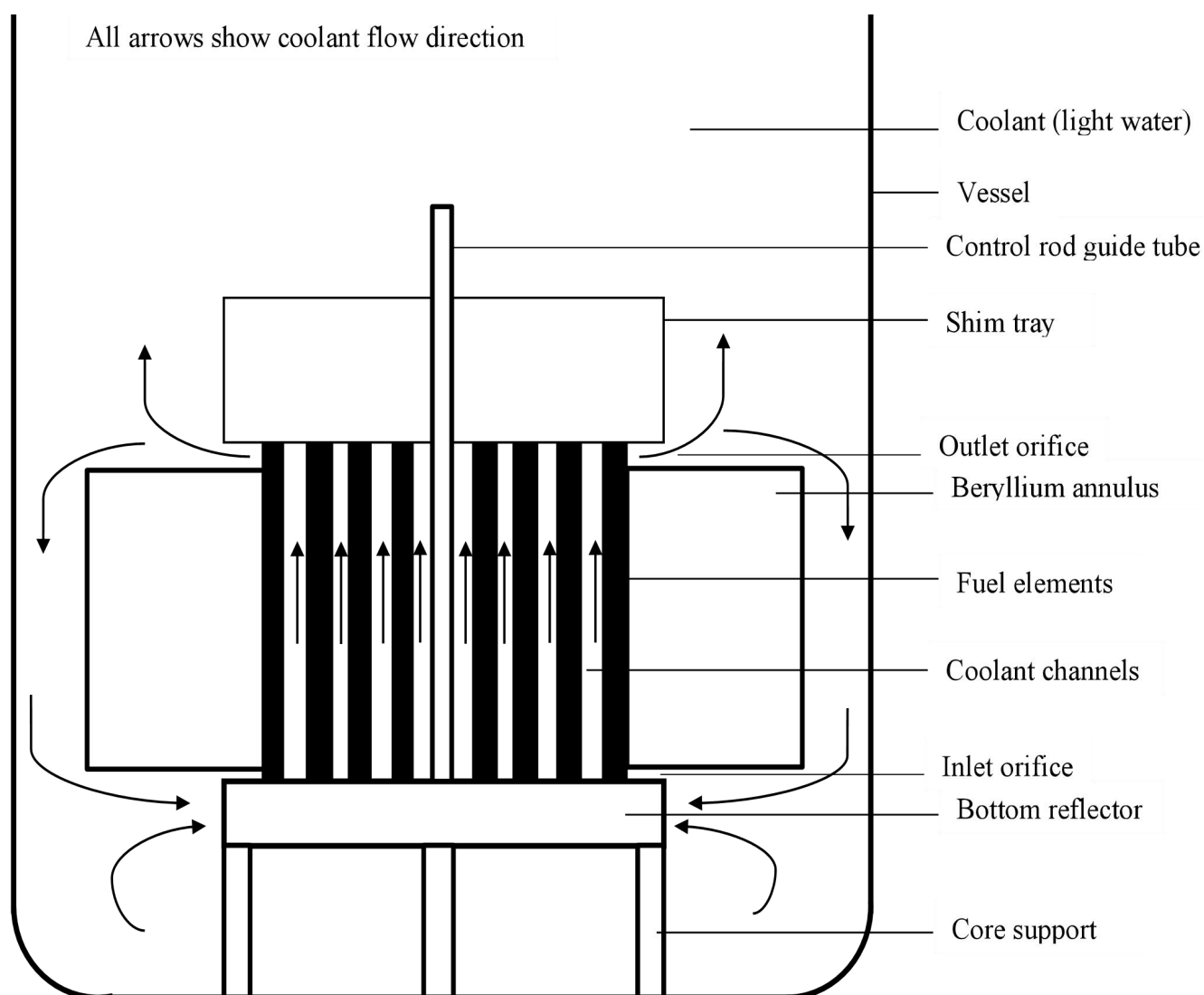

Figure 2: Sketch of natural circulation coolant flow pattern in MNSR

2.2   Fuel element model

The MNSR fuel element is depicted in Figure 3 with dimensions in mm. the labels are described as: 1. Top end plug (Al alloy); 2. Gap between fuel meat and clad; 3. Clad (Al alloy); 4. Fuel pellet (U-Al alloy); 5. Lower end plug (Al alloy). The core of MNSR contains 350 fuel elements lattices or positions, and some of few positions are filled with dummy fuel elements. The number of dummies differ from one MNSR to another. NIRR-1 core has 347 fueled elements and 3 dummies which are distributed evenly in the core. The model in Figure 4 shows the structure of the fuel element with the gap in-between the pellet and clad where rc is the clad radius from the fuel centre line, rf is the fuel pellet radius, and d is the gap width.
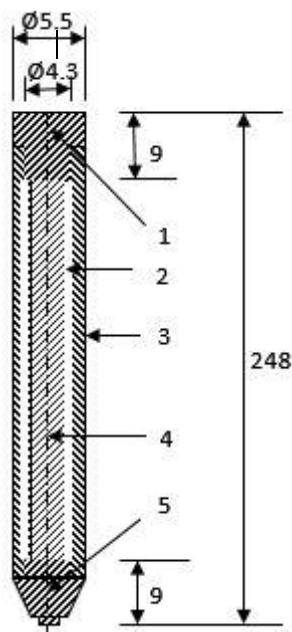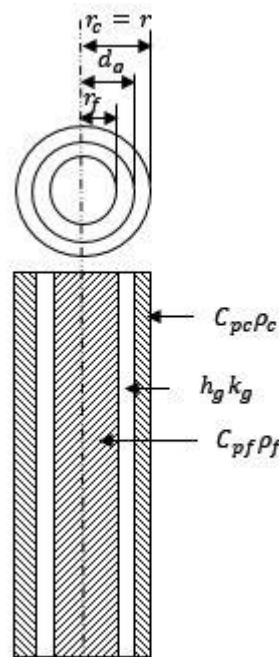
Figure 3: MNSR fuel element diagram

Figure 4: MNSR fuel element model

Heat is transferred through the fuel pellet to its surface with the gap by conduction, then through the gap to the inner surface of the clad by radiation since the gap does not contain any fluid, then pass through the clad to the outer clad surface by conduction and then to the coolant by convection and radiation at the clad surface. In a simplified lumped parameter formulation (Kazeminejad, 2008), for cylindrical fuel elements immersed in a coolant given the assumptions that there is azimuthally uniform fuel to clad conductance; there is no azimuthal variation of fuel heat generation; there is uniform clad to coolant heat transfer; and no axial heat flow along the fuel element. Eq. (1) and (2) are the partial differential equations for the diffusion of heat within each fuel element in the reactor core region in time domain were reduced to Eq. (3) and (4) are the required boundary conditions.

For fuel region;

$$C_{pf}\rho_f \frac{\partial T_f}{\partial t}(r, t) = \frac{1}{r}\frac{\partial}{\partial r}\left[K_{fm}r\frac{\partial T_f}{\partial r}(r, t)\right] + q_v(r, t) \tag{1}$$

and for the cladding region, it is expressed in the form;

$$C_{pc}\rho_c \frac{\partial T_c}{\partial t}(r, t) = \frac{1}{r}\frac{\partial}{\partial r}\left[K_c r\frac{\partial T_c}{\partial r}(r, t)\right] \tag{2}$$

The required boundary conditions may be reduced to Eq. (3) and (4);

$$K_c \frac{\partial T_c}{\partial r}(r, t)\bigg|r = r_c = h\,(T_c - T_f) \tag{3}$$

$$K_{fm}r\frac{\partial T_f}{\partial r}(r, t)\bigg|T = T_{fm} = K_c \frac{\partial T_c}{\partial r}(r, t)\bigg|r = r_{fm} \tag{4}$$

where: C_{pf} is heat capacity for the fuel element, C_{pc} is heat capacity for the cladding, k_{fm} is thermal conductivity of fuel meat, k_c is thermal conductivity of cladding, T_c is clad surface temperature, T_f is fuel pellet surface temperature, q_v is the volumetric heat generation rate, r_f is the fuel pellet radius, r_c is the clad radius, and T_f and T_c are the fuel and clad average temperatures respectively.

2.3 Modified thermal hydraulic model

Considering the heat transfer process in the reactor fuel element from the fuel pellet through the gap to the clad based on the afore mentioned assumptions and average temperatures of the fuel and clad, Eq. (1) and (2) with the conditions in Eq. (3) and (4) can be simplified to yield 1st order ordinary differential equations (5) and (6).

$$C_f \frac{dT_f}{dt} = \frac{Q_1}{A_f} - \frac{(T_f - T_c)}{R_f} - Q_{rg} \tag{5}$$

$$C_c \frac{dT_c}{dt} = \frac{(T_{f-} T_c)}{R_f} - \frac{(T_c - T_b)}{R_c} - Q_{rc} \tag{6}$$

where;

$$C_f = \pi r_f^2 C_{pf} \rho_f \tag{7}$$

$$C_c = 2\pi r_c (r_c - r_f) C_{pc} \rho_c \tag{8}$$

$$R_f = \frac{1}{4\pi k_f} \tag{9}$$

$$R_c = \frac{1}{2\pi r_c h} \tag{10}$$

$$Q_{rg} = \frac{\sigma \, \varepsilon_f \, \varepsilon_c}{\varepsilon_f + \varepsilon_c - \varepsilon_f \varepsilon_c} \frac{\left(T_f^4 - T_c^4\right)}{(T_f - T_c)} \tag{11}$$

$$Q_{rc} = \sigma A_c \left(T_c^4 - T_b^4\right) \tag{12}$$

$$h = \frac{k}{D_h} n(Gr\ Pr)m \tag{13}$$

where: C_f is the thermal capacity of fuel pellet (W/mK), C_c is the thermal capacity of clad (J/mK), R_f and R_c are the resistances between fuel pellet and gap, and between clad and coolant respectively (mK/W), h is the heat transfer coefficient for natural convection in fuel rod bundles (W/m^{2}K), Q_1 is the reactor power (W), A_f is the average cross section of the fuel (m^2), Ac is the clad surface cross-section, ε_f and ε_c are the fuel and clad surfaces emissivity, Q_{rg} is the rate of heat transferred at gap by radiation (W), Q_{rc} is the rate of heat transferred from clad surface by radiation (W), $\sigma = 5.67 \times 10^{-8}$ W/m^{2}K^4 (Stefan-Boltzmann constant), k is the thermal conductivity of the coolant (light water), Dh is the hydraulic diameter or equivalent length (m), and Gr and Pr are Grashof's and Prandtle's numbers respectively. The constants n and m for MNSR have been determined (Zhang, 1993, Wuqin, 1997) where;

n = 0.68, m = 1/4, for Gr. Pr < 6 × 10^6 (laminar flow)

$$n = 0.174, m = 1/3, \text{ for Gr. Pr} \geq 6 \times 10^6 \text{ (turbulent flow)} \tag{14}$$

The heat transfer and exchange in the core, from the fuel element clad to the core coolant and the pool is obtained by conservation of momentum and energy balance based on the average flow velocities and temperatures in the various regions and heat is supposed to transfer only radially. The lumped parameter method is most suitable for this type of transients. For MNSR diagram presented in Figure 5 and having a coolant flow pattern as depicted in Figure 6, the reactor is segmented in to regions as follows: R_1 is the fuel elements region in core, R_2 is the reflector, R_3 is the reactor vessel region above the core, R_4 is the bottom reflector region, R_5 is the reflector shim (tray) region, R_6 is the down-comer region between the side reflector and vessel wall where the downward movement of the coolant occurs due buoyancy in the circulation process and R_7 is the reactor pool. The governing equations of heat transfer process as shown in Figure 6 for the entire reactor system can be written as follows:

$$HC_{pb}\rho_b \frac{dT_b}{dt} = \frac{A_c}{A_f}h_c\,(T_c - T_b) - C_{pb}U_b\rho_b(T_2 - T_1) - Q_2 \tag{15}$$

$$2(H + H_1)\,\rho_b \frac{dU_b}{dt} = gH\,(\rho_1 - \rho_b) + gH_1(\rho_1 - \rho_2) - \Delta P \tag{16}$$

$$M_1 C_p \frac{dT_1}{dt} = A_{dc}C_p U_{dc}\rho_3(T_3 - T_1) + Q_2 - Q_{2b} - Q_3 \tag{17}$$

$$T_2 = 2T_b - T_1 \tag{18}$$

$$M_3 C_p \frac{dT_3}{dt} = A_f C_p U_b\rho_b(T_2 - T_1) - A_{dc}C_p\rho_b U_{dc}(T_3 - T_1) - Q_4 - Q_6 \tag{19}$$

$$M_4 C_p \frac{dT_4}{dt} = Q_{2b} - Q_5 \tag{20}$$

$$M_5 C_p \frac{dT_5}{dt} = Q_5 - Q_{35} - Q_9 \tag{21}$$

$$M_6 C_p \frac{dT_6}{dt} = Q_3 - Q_{34} - Q_{35} - Q_8 \tag{22}$$

$$M_7 C_p \frac{dT_7}{dt} = Q_4 + Q_{34} - Q_7 \tag{23}$$

where: H (m) is the reactor core height, H_1 (m) is the coolant height above the core, C_p is the average specific heat of coolant (J/kg K), ρ is the coolant average densities (kg/m^3), U is coolant averages velocity (m/s), g is the acceleration due to gravity (m/s^2), T denotes average temperatures (°C) depending on regions, ΔP is the pressure drop across the core, A is the cross sectional area, M is coolant mass (kg) and Q denotes heat transfers (w/m^{2}k) defined by Eq. (29) to (35). The subscripts c refers to clad; b refers to bulk coolant in the core; dc refers to down comer; and the numbers refer to the various positions shown in Figure 6.

ΔP is defined by Eq. (24) with the friction factor given in Eq. (25) as a function of the Reynold's number (Re) which is also defined in Eq. (26) and μ is the coolant average viscosity (Ns/m^2). The frictional drag coefficient (ξ) for flow in the coolant channel is in the form given in Eq. (27) which considers the core grid plate (Albarhoum and Mohammed, 2009) with 'a' denoting a geometric factor with average value of 0.45, and d_1 and d_2 denoting the equivalent diameter of the coolant sub-channels below and above the grid plate respectively. Eq. (28) expresses the coolant flow velocity at the down comer.

$$\Delta P = \left[\frac{FH}{2D_h} + \frac{\xi}{2}\right]\rho_b U_b^2 \tag{24}$$

$$F = \frac{64}{Re} \tag{25}$$

$$Re = \frac{\rho_b U_b D_h}{\mu_b} \tag{26}$$

$$\xi = a\left[1 - \left(\frac{d_2}{d_1}\right)^2\right] \tag{27}$$

$$U_{dc} = \frac{\rho_2 U_b A_c}{A_{dc}\rho_1} \tag{28}$$

In Figure 6, Q_1 is the reactor power, Q_2 is the rate of heat transferred from the coolant in the reactor core to the annulus Beryllium reflector by convection through the reflector by conduction to the coolant in the middle of the vessel by convection, Q_3 is the rate of heat transferred from the middle of the vessel to the middle of the pool, Q_4 is the rate of heat transferred from the upper part of the vessel to the upper part of the pool, Q_5 refers to the rate of heat transferred from the lower part of the vessel to the lower part of the pool, Q_{2b} is the rate of heat transferred from the upper part to the middle of the vessel, Q_{34} is the rate of heat

transferred from the upper part to the middle of the pool and Q_{35} is the rate of heat transferred from the middle part to the lower of the pool. Q6 is the rate of heat transferred to the chiller which absorbs heat through the coiled pipe wound at the upper part of the reactor vessel in the pool, Q_7 is the rate of heat transferred from the upper part of the pool to the pool wall, Q_8 is the rate of heat transferred from the middle of the pool to the pool wall and Q_9 is the rate of heat transferred from the lower part of the pool to the pool wall. Q_6 is described as the chiller (cooling coil) power in (W).

$$Q_2 = A_2 h_2 (T_b - T_2) \tag{29}$$

$$Q_3 = A_6 h_6 (T_1 - T_6) \tag{30}$$

$$Q_4 = A_7 h_7 (T_3 - T_7) \tag{31}$$

$$Q_5 = A_5 h_5 (T_4 - T_5) \tag{32}$$

$$Q_{2b} = A_{2b} h_{2b} (T_3 - T_1) \tag{33}$$

$$Q_{34} = A_{34} h_{34} (T_6 - T_7) \tag{34}$$

$$Q_{35} = A_{35} h_{35} (T_6 - T_5) \tag{35}$$

The time for linear power rise from zero to the selected value termed as Reactor Power Establishment Time (RPET) of NIRR-1 is not less than 300 seconds and is estimated experimentally in this work. Eq. (36) described the function that relate rising Reactor Power (RP) and RPET.

$$Q_1(t) = \frac{RP}{RPET} t, \text{for t } 0 \leq t \leq RPET \text{ and } Q_1(t) = RP, \text{for t} \geq RPET \tag{36}$$

Figure 5: MNSR diagram

Figure 6: MNSR thermal hydraulic model for natural convection
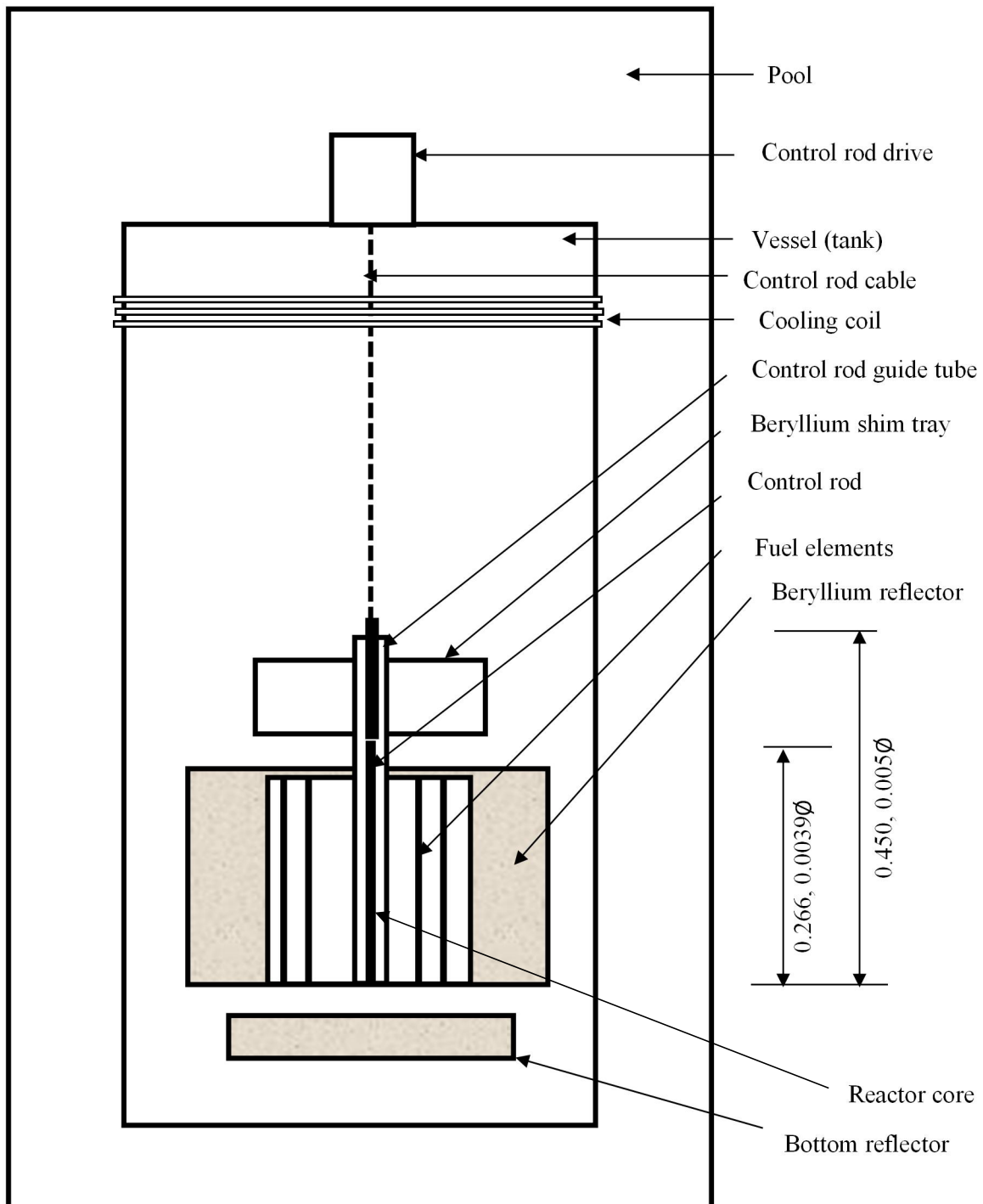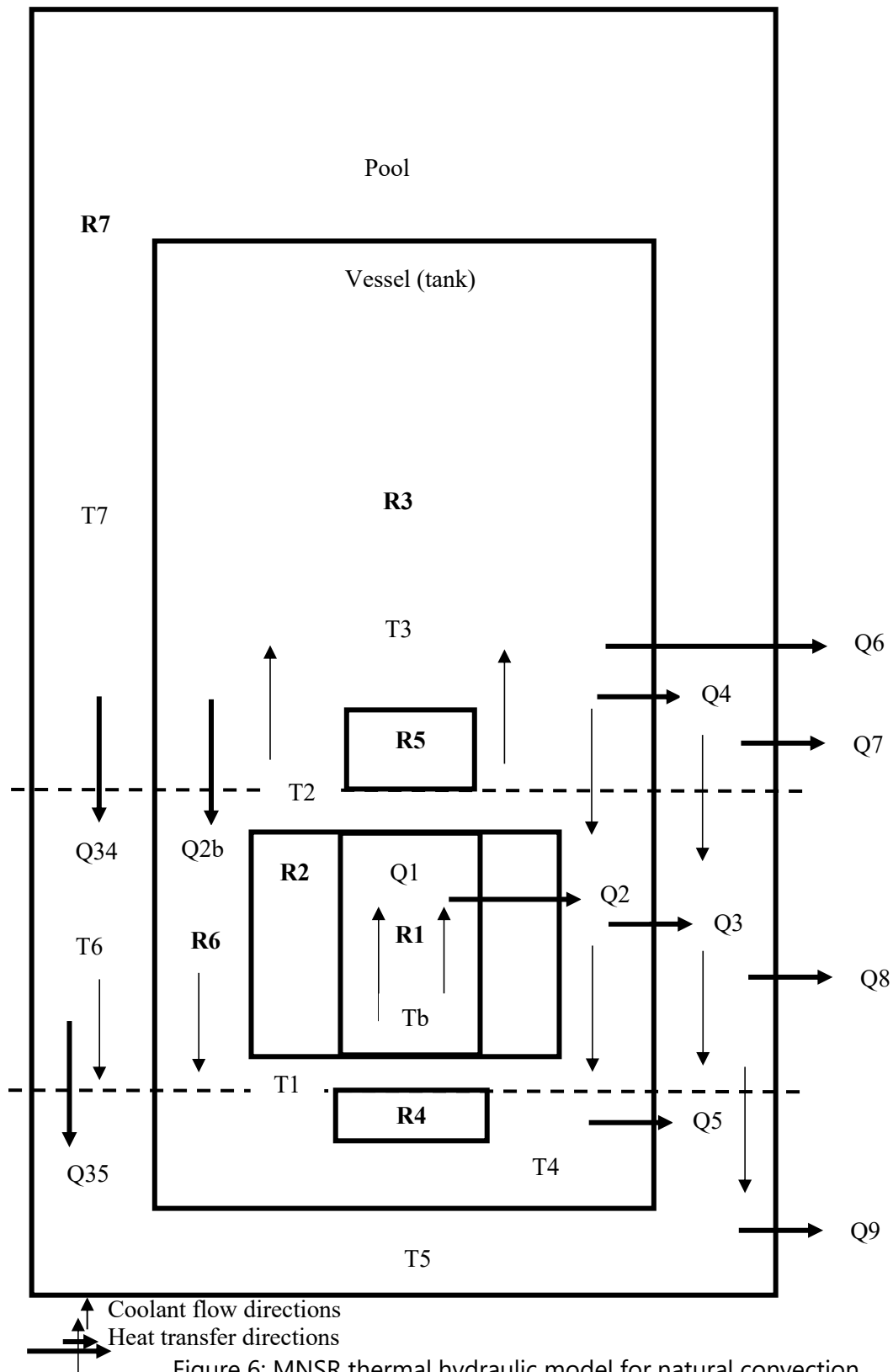
The lumped perimeter model formulated in this review constitutes the solution of the transient thermal hydraulic heat transfer problem of the MNSR. In this model, transient behaviour of the reactor is observed by the variations of eleven essential parameters involved; namely: T_f, T_c, T_b, T_1, T_2, T_3, T_4, T_5, T_6, T_7, and U_b. Where T_3, T_4, T_5 and T_6 denote the temperatures at the various

regions as shown in the Figure 6, T_7 denotes the average pool temperature, while U_b is denotes the coolant flow velocity. The system of equations from Eq. (5) to (35) were coupled together and solved numerically using MATLAB solver for variable order method in stiff differential equations and Differential-Algebraic equations (Shampine, et al., 1999, Endre, 2014), coupled with Maplesoft software.

3.   Results and discussion

NIRR-1 was nominally operated at 31 kW for about six hours without chiller which gives the data recorded in Table 1. The reactor power begun to decline at about four and half hours of operation and the reactor was then shutdown. The operation of the reactor was also carried out with the chiller being operated as recorded in Table 2 and the reactor was shut down just before the reactor begun to decline. The core average temperature T_b presented in the Tables referred to the coolant bulk temperature in the core and is computed using Eq. (18). The chiller installed capacity for NIRR-1 is 4000 Kcal/hr. which is equivalent to about 5000 W. From the experimental data, the RPET necessary for the power to reach its steady operational level was measured to be about 300s from the reactor startup. The core inlet and outlet as well as the pool temperatures were measured using the monitoring and control systems. There is limited instrumentation available to measure other important parameters. These parameters can only be estimated by simulation.

Table 1: Reactor Core thermal hydraulics parameters recorded during operation at 31 kW without chiller

Time (s)	Inlet Temperature, T_1 (^{o}C)	Outlet Temperature, T_2 (^{o}C)	Core Average Temperature, T_b (^{o}C)	Pool Temperature, T_7 (^{o}C)
0	23.00	23.40	23.20	25.50
720	24.30	41.60	32.95	25.50
1440	26.70	47.00	36.85	25.50
2160	29.70	49.50	39.60	25.70
2880	31.80	48.00	39.90	26.00
3600	32.90	52.30	42.60	26.10
4320	33.80	52.80	43.30	26.30
5040	34.40	53.60	44.00	26.60
5760	34.00	54.20	44.10	26.60
6480	34.30	54.70	44.50	26.80
7200	35.90	54.30	45.10	27.00
7920	36.20	55.20	45.70	27.30
8640	36.30	55.40	45.85	27.40
9360	36.70	55.70	46.20	27.50
10080	36.00	55.80	45.90	27.80
10800	36.50	56.00	46.25	28.10
11520	36.50	56.20	46.35	28.20
12240	36.70	55.10	45.90	28.40
12960	36.70	56.80	46.75	28.50
13680	36.80	56.60	46.70	28.80
14400	36.70	56.50	46.60	28.90

15120	37.50	57.00	47.25	29.20
15840	37.40	56.90	47.15	29.20
16560	37.40	57.00	47.20	29.40
17280	36.00	56.80	46.40	29.40
18000	33.90	36.70	35.30	29.70
18720	31.40	33.80	32.60	29.70
19440	29.70	32.00	30.85	29.80
20160	28.90	30.80	29.85	30.00
20520	28.40	30.60	29.50	30.00

Table 2: Reactor Core thermal hydraulics parameters recorded during operation at 31 kW with chiller

Time (s)	Inlet Temperature, T_1 (°C)	Outlet Temperature, T_2 (°C)	Core Average Temperature, T_b (°C)	Pool Temperature, T_7 (°C)
0	24.40	26.63	25.51	25.70
300	24.81	45.18	34.99	25.71
1200	27.10	47.31	37.20	25.71
2400	30.44	50.19	40.31	25.71
3600	32.74	52.32	42.53	25.73
4800	34.48	53.80	44.14	26.33
6000	35.38	53.90	44.64	26.34
7200	35.37	54.95	45.16	26.39
8400	36.10	55.40	45.75	26.52
9600	36.69	55.96	46.32	26.71
10800	36.60	55.80	46.20	26.76
12000	36.26	56.08	46.17	26.88
13200	37.30	56.80	47.05	27.07
14400	36.90	55.50	46.20	27.32
15600	37.10	57.20	47.15	27.60
16800	37.90	57.20	47.55	28.27

The system of equations formulated in describing the model used in this work was solved to produce the simulated time behaviour of the reactor parameters. T_1, T_2, T_b, T_7, T_f, T_c and U_b are the most important thermal hydraulic parameters of interest in the MNSR (Dim et al., 2012). The simulation outputs produced were tested by comparing the results to the experimental data to validate the model. In Figures 7, 8, 9 and 10, the inlet, outlet, bulk (core average) and pool temperatures from Table 1 are compared with the simulation outputs for T_1, T_2, T_b, and T_7 respectively. These were computed at the instance when Q_6, Q_7, Q_8 and Q_9 are equal to zero. This means that the chiller power was zero, thus, there was no heat exchange between the coolant and cooling coil. Therefore, the heat transferred from the core was only sunk in the pool. Figure 11 illustrates the simulated behaviours for T_f and T_c at 31 kW without applying the chiller.

At reactor startup, T_f and T_c had the same initial condition and begun to separate at about 40 °C in few seconds (Figure 11) and maintained a maximum difference in-between of about 3 °C. This difference aroused from the tiny gap (clearance) between fuel pellets and clad which

accumulates gases like xenon which could produce some resistance to heat transfer during operation. U_b was raised from in initial value (Table 3) to a maximum of about 0.012 m/s after few seconds from the reactor startup and was maintained until the reactor was shut down. The transient behaviours in Figures 7 and 11 has exhibited identical pattern by falling at about 4 hours 30 minutes in both experimental and simulated results. The fall in temperatures observed during operation can be largely attributed to the rising temperature effect which slows down the fission reaction in the fuel (Doppler effect). This makes the reactor power to also fall (Albarhoum and Mohammed, 2009, Anglart, 2011, Abubakar and Yahaya, 2012). The RPET was also observed to be 300s from reactor start-up to the pre-set value of 31 kW during the simulations.

It can be noticed in Figures 7, 8, 9 and 10 that good agreement is achieved between the model predictions and the experimental results. The sharp fall of the temperatures in the experimental data as plotted against the simulation outputs were due to the deliberate reactor shutdown. It can be observed that both experimental and simulated T_1 begun to decline at the same time in Figure 7. The behaviour exhibited by the model follows the same trends as plotted with the experimental data up to the maximum time of about 16,700s (5 hrs.) known for steady stable MNSR operation. In Figures 7, 8, 9 and 10, the average difference or error between recorded data and simulated result is 3%. Based on the aforementioned agreements between the experimental and simulation outputs, the model was used to simulate T_f, T_c, U_b and the influence of the chiller at different power levels.

The influence of varying the chiller (cooling coil) power Q_6, on various temperatures in the reactor was analysed at different cooling coil powers. The position of the cooling coil is shown in Figure 5 and its rate of heat transfer is represented by Q_6 in Figure 6. Table 2 shows the record obtained when the chiller was operated during reactor operation. The results recorded showed no significant difference in values with or without chiller except in the pool average temperature which was noticed to have reduced by about 1°C. Table 3 shows the variation of reactor transient thermal hydraulic parameters at various chiller powers. It is noticed that the installation of cooling coil of the chiller system at the at the upper part of the reactor pool (present position) would have no advantage on the core cooling.

Table 3: Computed thermal hydraulic parameters at different chiller powers (This work)

Parameter	Minimum (initial) values at 0.0 s	Maximum average values computed at (270 minutes) 16200 s					Maximum average values when the chiller cooling coil is position at the core area at (270 minutes) 16200 s
T_f (°C)	24.57	65.68	65.62	65.56	65.44	65.22	63.90
T_c (°C)	24.57	63.22	63.16	63.09	62.97	62.76	60.87
T_b (°C)	23.20	47.64	47.56	47.49	47.34	47.05	45.55
T_1 (°C)	23.00	36.84	36.79	36.75	36.66	36.48	34.24
T_2 (°C)	23.40	58.44	58.33	58.23	58.02	57.62	56.86
T_7 (°C)	24.57	29.20	25.67	25.66	25.63	25.58	25.72
U_b (m/s)	0.0100	0.0118	0.0118	0.0118	0.0118	0.0118	0.01178
Chiller power, Q_6 (kW)	0.0	30	60	120	240	Installed power (5 kW)	

Comparing Tables 1 and 2, when the chiller was operated at the installed capacity of 5000 W, only the pool temperature was slightly affected by reduction at a magnitude of about 2 °C. Table 3 gives the summary of the simulation outputs computed by adjusting the chiller power from 0 to 240 kW at 30 kW interval. An insignificant decrease was noticed at all maximum values of the reactor thermal hydraulic parameters with increase in the chiller power, except for the pool temperature which notably shows a reduction from 29.20 °C to 25.67 °C at 30 kW (a difference of about 4°C). If increase in the chiller power (up to about four times the reactor power) is compared with the decrease in the maximum temperature values recorded, the effect of the cooling coil is relatively insignificant.

When the cooling coil position was changed to the core area R6 in Figure 6 and equating Q_6 to the install chiller power of 5 kW, a significant change was observed by reduction in T_f, T_c, T_b, T_1 and T_2

at a magnitude of about 2 °C. The core coolant flow velocity was not affected by the change in the chiller power. It remains constant when it reached its maximum value of 0.0118 m/s in all the cases shown in Table 3. The simulation outputs reassured that there would not be efficient heat transfer in the core. Therefore, if efficient core cooling is required in the MNSR core, the present position of the cooling coil has to be considerably changed to a position below the current one closer to the core region R6.
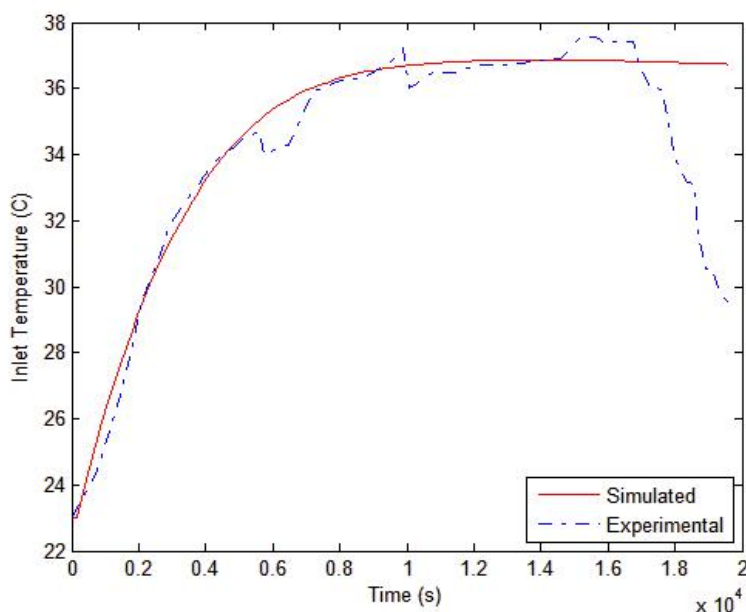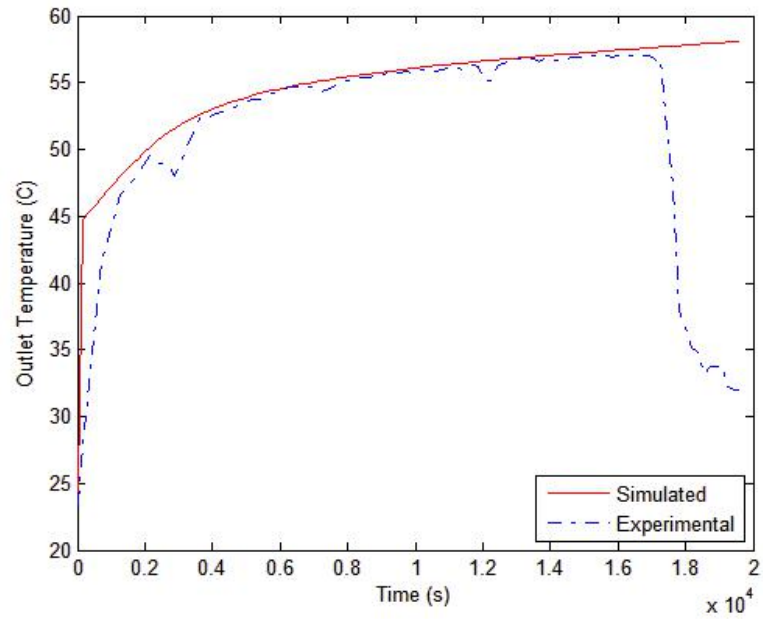

Figure 7: Inlet temperature (T_1) variation

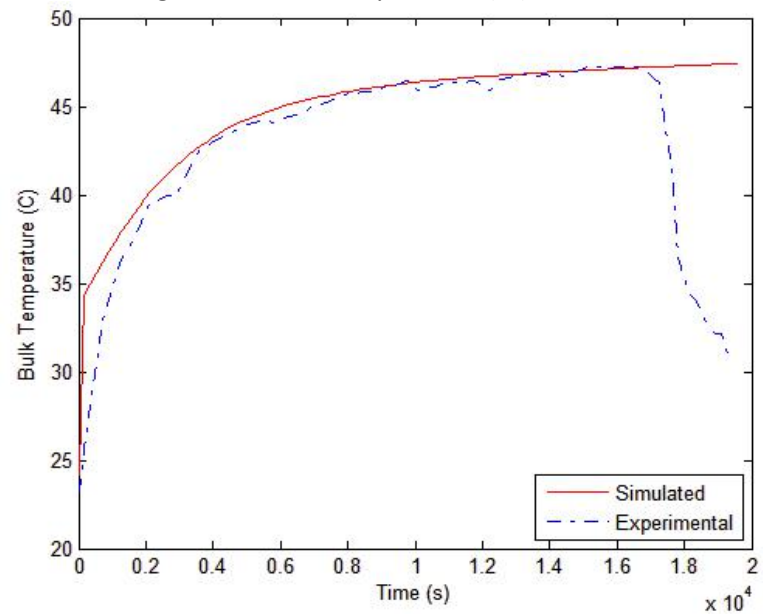Figure 8: Outlet temperature (T_2) variation

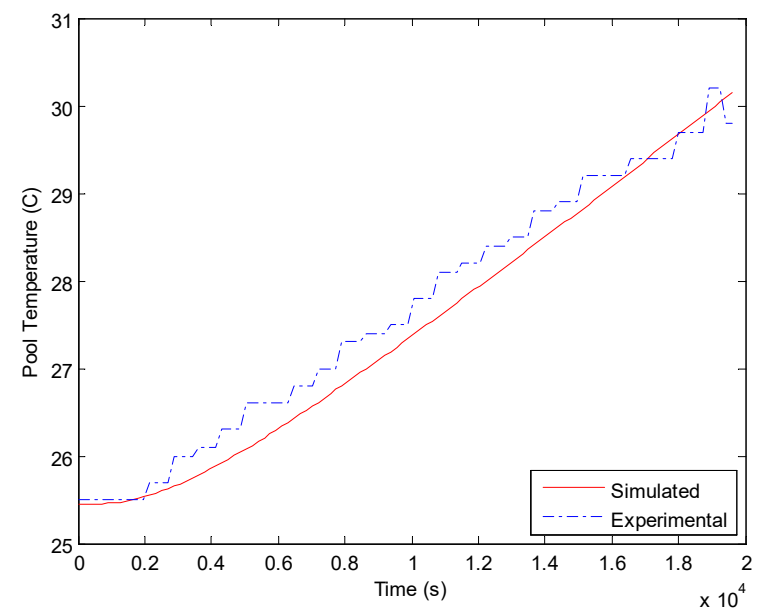Figure 9: Bulk (core average) temperature (T_b) variation

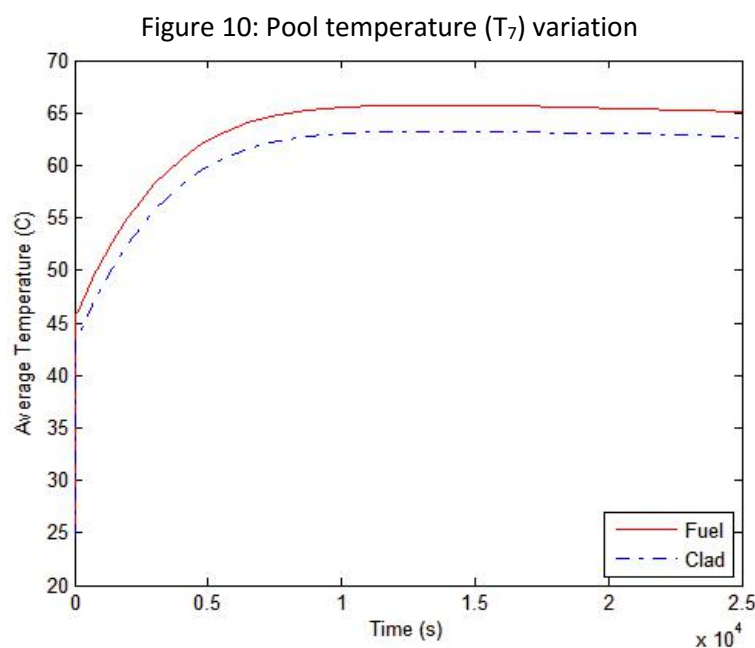Figure 10: Pool temperature (T_7) variation

Figure 11: Fuel (T_f) and Clad (T_c) average temperatures variation

4. Conclusion

A model based on lumped parameter method is presented to predict the thermal hydraulic behaviour of the MNSR and validated using NIRR-1 facility configuration. The model is capable of predicting flow velocity and the fuel and clad temperatures. It can be used of to simulate the reactor operation with or without operating the cooling coil and can also predict the reactor behaviour by changing the position of the cooling coil. Both transients and beginning of steady state conditions can be predicted.

The fuel and clad temperatures exhibited the same pattern as expected but begun to differ in transient until the difference rieaches a steady maximum of about 3 °C. This is at the instance of the gaseous accumulation in fuel tube during operation as a result of the fission reaction. Xenon gas was considered as the major gas produced from fission during transients. When the cooling coil was repositioned to the core area at installed capacity of 5 kW, the computation shows a significant improvement with temperatures' decrease in magnitude of about 2°C. Thus, the chiller would be more effective if installed at the middle section of the pool.

In the present work, the model is used to predict variations in eleven reactor parameters and to study the effect of cooling the reactor from the pool upper section by the installed chiller at different powers. This study finds experimentally and by simulation at different chiller power, that the effect of cooling the reactor at the pool upper section is insignificant in the reactor core. And whenever the reactor fuel is changed in the future as intended, only the fuel parameters are required to be changed in the model.

References

Abubakar, N. and Yahaya, DB. 2012. An Overview of Thermal Hydraulic Behaviour of the First Nigeria Nuclear Research Reactor (NIRR-1) Manifesting to Its Inherent Safety. Journal of Engineering and Technology, 7(1-2): 29-33.

Albarhoum, M. and Mohammed, S. 2009. A thermal-hydraulic code (THYD) for the miniature neutron source reactor thermal-hydraulic transients. Progress in Nuclear Energy, 51: 470-473.

Anglart, H. 2011. Nuclear Reactor Dynamics and Stability; Compendium [program] KTH Research Reactor Project. Stockholm: Royal Institute of Technology.

Dim, L., Usman, K., Balogun, G., Mallam, S., Ewa, I., Funtua, I., Yusuf, I., Mati, A. and Ogunleye, P. 2012. Nigeria Research Reactor - 1 Safety Analysis Report. Zaria: Centre for Energy Research and Training CERT.

International Atomic Energy Agency, IAEA. 2001. Reactor Simulator Development. Technical Document TECDOC-1203. Vienna: IAEA.

Endre, S. 2014. Numerical Solution of Ordinary Differential Equations. Mathematical Institute. Oxford: University Press.

Kazeminejad, H. 2008. Thermal-hydraulic modelling of flow inversion in a research reactor. Annal of Nuclear Energy, 35: 1813-1819.

Saha, P., Aksan, N., Andersen, J., Yan, J., Simoneau, P., Leung, L., Bertrand, F., Aoto, K. and Kamide, H. 2013. Issues and future direction of thermal hydraulics research and development in nuclear power reactors. Nuclear Engineering and Design, 264: 3-23.

Shampine, LF., Reichelt, MW. and Kierzenka, JA. 1999. Solving Index-1 DAEs in MATLAB and Simulink. SIAM Review, 41: 538–552.

Yamoah, S., Akaho, EHK., Nyarko, BJB., Asamoah, M., Ampong, AG. and Amponsah-Abu, EO. 2011. Analysis of thermal-hydraulic transients for the Miniature Neutron Source Reactor (MNSR) in Ghana. Research Journal of Applied Sciences, Engineering and Technology, 3(8): 737-745.

Quian, S. 1990. Design of Fuel Elements for Low Power Research Reactors. IAEA Workshop on Low Power Research Reactors. Beijing: China Institute of Atomic Energy.

Wuqin, Z. 1997. Dynamic characteristics of the Miniature Neutron Source Reactor. Technical Document. Beijing: China Institute of Atomic Energy.

Yongchun, G., Jijin, G., Huabai, T. and Yuewen, Y. 1992. Miniature Neutron Source Reactor General Descriptions, MNSR-DC-1. Technical Document. Beijing: China Institute of Atomic Energy.

Zhang, Y. 1993. The Whole Simulated Heat Transfer Experiment and Calculations. MNSR Training Materials. Beijing: China Institute of Atomic Energy